

See discussions, stats, and author profiles for this publication at: <https://www.researchgate.net/publication/283215225>

# Segmentation of carbon nanotubes through an artificial neural networkk

Conference Paper · October 2015

DOI: 10.1007/978-3-319-27060-9\_28

---

CITATIONS

3

READS

143

4 authors:



Celeste Ramirez

Center for Research and Advanced Studies of the National Polytechnic Institute

2 PUBLICATIONS 12 CITATIONS

[SEE PROFILE](#)



Teresa Alarcón

University of Guadalajara

23 PUBLICATIONS 149 CITATIONS

[SEE PROFILE](#)



Oscar S Dalmau-Cedeño

Centro de Investigación en Matemáticas (CIMAT)

56 PUBLICATIONS 194 CITATIONS

[SEE PROFILE](#)



Adalberto Zamudio-Ojeda

University of Guadalajara

30 PUBLICATIONS 661 CITATIONS

[SEE PROFILE](#)

Some of the authors of this publication are also working on these related projects:



Diabetic Retinopathy Detection using Image Processing [View project](#)



Characterization of carbon nanotube through digital image processing [View project](#)

# Segmentation of carbon nanotube images through an artificial neural network

María Celeste Ramírez Trujillo<sup>1,\*</sup>, Teresa E. Alarcón<sup>2</sup>, Oscar S. Dalmau<sup>3</sup>, Adalberto Zamudio Ojeda<sup>4</sup>

<sup>1,4</sup>Universidad de Guadalajara, Jalisco, México

teresa.alarcon@profesores.valles.udg.mx

nanozam@gmail.com

<sup>3</sup>Centro de Investigación en Matemáticas, Guanajuato, México

dalmau@cimat.mx

**Abstract.** The segmentation of nanotube is an important task for Nanotechnology. The performance of segmentation stage determines the accuracy of the measurement process of nanotube when assessing the quality of nanomaterials. In this work we propose two algorithms for segmenting carbon nanotube images. The first one uses a matched filter bank in the preprocessing step and a neural network for segmenting images from Scanning Electron Microscopy. The second algorithm includes the Perona-Malik filter for enhancing the nanotube information. The segmentation phase is composed by the relaxed Otsu's threshold and an artificial neural network. This algorithm is applied on images from Transmission Electron Microscopy. After the segmentation, for both algorithms, a preprocessing based on mathematical morphology is carried out. The performance of the proposed algorithms is numerically evaluated by using real image databases. Overall accuracy of 92.74 % and 73.99 % were obtained for the first and second algorithm respectively.

**Keywords:** segmentation, artificial neural network, filter bank, thresholding.

## 1 Introduction

Carbon nanotubes (CNT) are tubular structures with nanometric dimensions which are studied by nanoscientists and nanotechnologists. The dimensions of the nanotube, in particular the diameter, determine its electrical, mechanical and thermal properties. Depending on their properties, nanotubes are used in different fields of industry, electronics and biology [21]. In order to measure the characteristics of nanotubes, nanotechnologists need to spend much time [1]. The analysis results vary considerably from one specialist to another and there are accuracy problems. The use of computers leads to automatic or semiautomatic detection of the nanotube structures in digital images reducing the time effort and improving the accuracy of the analysis. Therefore, Nanoscience and

Nanotechnology have been favored with the use of computers. The detected nanotubes are measured using the computers [8]. The obtained measurements are usefully for characterization purposes.

There are several approaches for segmenting images using Digital Image Processing: thresholding [2] and clustering techniques [6], histogram methods [20], edge based segmentation [15], region growing techniques [16], and probabilistic approaches [9] among others [11]. Segmentation of tubular structures as nanotubes is a very difficult and time consuming task. In [4] the authors present a segmentation algorithm of the human karyotyping based on thresholding, edge linking and the laplacian operator. A similar problem is addressed in [19] through a Multidirectional Block Ranking algorithm. The segmentation of retinal vessel also engages the detection of tubular structures, this problem is addressed in [7] by combining a Matched filter bank with a cellular automata.

In this work we provide nanotube segmentation algorithms for images obtained from Scanning Electron Microscopy (SEM) and from Transmission Electron Microscopy (TEM). We face the main problems to segment both types of images: the nanotube overlaps, poor illuminations, and different artifacts that make it very difficult to segment the image. For TEM images the complexity increases due to the presence of the grid during the synthesis step, the noticeable similarity between nanotube and background zones and holes that could appear inside nanotubes. Therefore, the elaborated proposal includes an algorithm for segmenting SEM images and an algorithm for segmenting TEM images. Both algorithms consider three steps: preprocessing, segmentation and postprocessing. In the preprocessing step, we enhance the nanotube information by filtering the image. For SEM images we use a bank of matched filters [7,13] and for TEM images, the Perona-Malik approach [18]. The segmentation of SEM images uses a neural network trained with samples of intensity levels of nanotube and background regions. The segmentation of TEM images is achieved by means of two phases: firstly an automatic Otsu's threshold [17] is computed and then is relaxed. This phase results in three classes: CNT, background and uncertainty zone. In the second phase a neural network is trained taking into consideration the homogeneity, the energy, the correlation and the intensity levels of pixels falling in CNT and background classes. The homogeneity, energy, contrast and correlation are computed from cooccurrence matrix [12]. During the generalization stage the neural network classifies the pixels in uncertainty zone. The complexity of TEM images leads to design a specific neural network for each TEM image to be analyzed. After the segmentation of both kinds of images follows a preprocessing step through morphological operators. The segmentation results are compared with manually-segmented images by an expert. The overall accuracy for SEM images was 92.74 %. When we considered a whole TEM image the overall accuracy was 73.99 %, in the case of analyzing a region of interest indicated by an expert the overall accuracy reaches the value of 84.07 %. The segmented images are used for characterization purposes by Nanotechnologists [1].

The structure of this manuscript is the following. Section 2 describes the images under study and two algorithms for segmenting CNT, one algorithm for each type of image. Section 3 explains and discusses the experimental work and finally, in Section 4 we present the conclusions.

## 2 Segmentation algorithm

### 2.1 Study images

The structure of a carbon nanotube is like a sheet of graphite rolled upon itself. There are different techniques for capturing images of carbon nanotubes. In this research the images under study are acquired using two techniques: Scanning Electron Microscopy (SEM) and Transmission Electron Microscopy (TEM)<sup>1</sup>. Fig. 2.1 shows examples of SEM and TEM images.

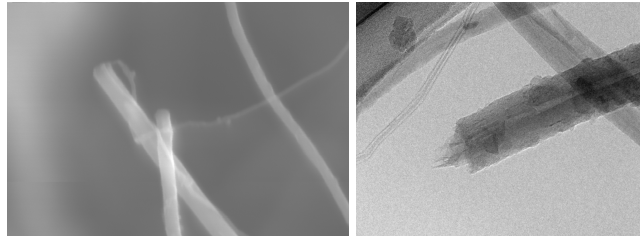


**Fig. 1.** Left : SEM carbon nanotube image. Right: TEM carbon nanotube image

In SEM images, pixels associated with nanotube information present a higher gray level, however, the intensity level distribution inside nanotube is not uniform. Furthermore, changes in brightness in the background cause confusion between nanotube and background. The overlaps of nanotubes on the edges cause a decreasing intensity and shadow areas. The lack of sharpness in the images makes difficult to find the exact delimitation between the background and the nanotube. Therefore, the edge information seems to be not useful for segmenting this type of images. On the other hand, TEM images also present some problematics that make them very hard to segment. They may contain elements other than carbon, for example, iron spots. Nanowires or nanoparticles can be found inside the tubes. In TEM images one can observe cavities with a trapezoid shape. In most cases, the intensity of cavities is very similar to the background of the image. The grid used for nanotube synthesis sometimes appears in the image, with a gray distribution similar to the nanotube. Certain TEM images may have

---

<sup>1</sup> The images used in this project were provided by Research and Development of Nanomaterials, SA CV RENIECYT 17567 ( National Registry of Scientific and Technological Institutions and Enterprises CONACYT), through MsC. Daniel Ramirez Gonzalez and funded by the PROMEP / 103.5 / 11/6834 project.

an artifact in the background, similar to the expansion of water waves. All these mentioned facts lead to changes in luminosity and deformation of nanotube edges, what makes a very difficult segmentation process. The above explanation justifies the elaboration of two algorithms: one for the segmentation of SEM images and the other one for TEM images.

## 2.2 Segmentation algorithm for SEM images

For SEM images we follow a semiautomatic segmentation approach. However, the previous idea is not applied directly on the original image. In our case, we take advantage of the geometry of the structure to be segmented, in particular, nanotubes are elongated structures. Hence, we propose the following segmentation steps for SEM images:

1. **Preprocessing.** In this step we transform the original image in order to enhance the nanotube information. For increasing the contrast between nanotube and non-nanotube (background) we propose to apply an appropriate filter bank. In this work we use a matched filter bank, see Refs. [5], [7], [13] for details. The filter bank is composed by a set of kernels with Gaussian profiles. First, a main kernel is built with cross section, or profile, based on a Gaussian function. The remaining kernels are obtained from the previous kernel by means of rotations and scale changes. The filter bank allows us to enhance the nanotube information and remove illuminance variations in the background of the image.
2. **Feature extraction.** As feature vector we simply use the maximum response of the Matched Filter Bank of pixels belonging to the regions of interest, i. e., nanotubes regions and background regions, because the maximum response provides a good contrast between nanotubes and non-nanotubes regions. Fig. 2 depicts an example of this part of the algorithm, in which a user selects the corresponding training set. Although we could be tempted to use a more sophisticated feature vector in order to get a good segmentation result, as we will see in the experiment section, the use of other local features does not guarantee a better result.
3. **Segmentation.** For the segmentation process, a multilayer perceptron (MLP) neural network was selected. Table 1 shows the configuration of the artificial neural network. The neural network was trained using the data set obtained in the previous step.
4. **Postprocessing.** Due to the problematics of SEM images the MLP could obtain nanotubes which are not well-defined, mainly with holes, or it could appear some granularity. These artifacts should be removed in order to obtain a good characterization of nanotubes. Therefore, in general, a post processing is required. All implemented operations are summarized below:
  - (a) *Removing holes and granularity.* For removing holes and granularities we simply use morphological operators of *closing* and *opening* with a structural element (SE) of type diamond, clearly the size of SE depends on the maximum size of hole needed to fill, in our case the parameters are

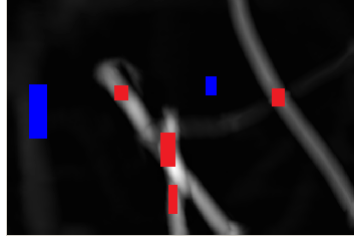


**Fig. 2.** Extraction of regions of interest. In red: samples of nanotube zones, in blue: samples of background regions

**Table 1.** Selected configuration for the multilayer perceptron. SEM images.

Number of layers	<i>1 hidden layer with 20 neurons</i>
Activation function in the hidden layer	<i>logistic sigmoid</i>
Activation function in the output layer	<i>Lineal</i>
Training algorithm	<i>Levenberg-Marquardt [3], [10], [14]</i>
Maximum number of iterations	<i>100</i>
Error validation function	<i>mse</i>
Gradient value	<i><math>10^{-4}</math></i>

obtained experimentally. To connect near objects and remove small holes, the closing operation is used with the structural element of diamond type with 6 pixels in diameter. Regions with less than 1500 pixels are removed by means of labeled components. Of course, a more pragmatic alternative could be to fill or remove ‘small holes’, for example: to identify regions with area less than 1 % with respect to the total size of the processed image, and again, the parameters can be experimentally calculated or trained.

- (b) *Edge smoothing.* Finally, with the goal of obtaining nanotube with smooth edges, a median filter of size 16x16 pixels is applied on the image obtained in the previous step.

### 2.3 Segmentation algorithm for TEM images

In the case of TEM images we present an automatic segmentation alternative. Although the idea is similar to the previous algorithm, we adapt it for TEM images because, as explained above, they have different characteristics. For example, we change the *preprocessing* step because the application of the Matched Filter bank does not produce good results.

1. **Preprocessing.** The general idea is to increase the contrast between nanotube and non-nanotube information, to remove noise and preserve the edge of nanotubes. For the previous reasons, we use the Perona-Malik [18] filter. The application of Perona-Malik algorithm allows us, at the same time,

to enhance the information of nanotubes in TEM images, to preserve the nanotube borders and attenuate noise.

2. **Segmentation.** Now we can find pixels that belong to nanotubes and background by means of Otsu's method [17]. Then, we can binarize the image by using the automatic threshold  $U$  computed with Otsu's. However, this simple idea does not yield good segmentation results. Instead, the threshold  $U$ , is relaxed by a certain value ( $\theta$ ), that leads to two new thresholds,  $U_1 = U - \theta$  and  $U_2 = U + \theta$ . Equation (1) explains how the two new thresholds are used on the segmentation process:

$$F(g(r)) = \begin{cases} \text{background} & \text{if } g(r) < U_1 \\ \text{nanotube} & \text{if } g(r) > U_2 \\ \text{uncertainty area} & \text{otherwise} \end{cases} \quad (1)$$

where  $g(r)$  represents the gray level of the pixel  $r$  in the image. Pixels with intensities greater than  $U_2$  have high confidence to belong to the nanotube region and are classified as nanotube, and pixels with intensities less than  $U_1$  have high confidence to belong to the background and are classified as non-nanotube. For classifying pixels with intensities in  $[U_1, U_2]$ , i.e., pixels with low confidence, we use a neural network. The training set is obtained by considering pixels with high confidence to belong to a class, as background or nanotube. As feature vector we use the homogeneity, energy, contrast and correlation which are computed based on the cooccurrence matrix, and also, the intensity levels of the image. Table 2 describes the artificial neural network used for segmenting the uncertainty region. It is important to note,

**Table 2.** Selected configuration for the multilayer perceptron. TEM images.

Number of layers	<i>1 hidden layer with 20 neurons</i>
Activation function in the hidden layer	<i>hyperbolic tangent sigmoid</i>
Activation function in the output layer	<i>Lineal</i>
Training algorithm	<i>Levenberg-Marquardt</i> [3], [10], [14]
Maximum number of iterations	<i>100</i>
Error validation function	<i>mse</i>
Gradient value	$10^{-4}$

that in the case of TEM images, the neural network is trained and applied for each particular image, due to the complexity of this type of images.

3. **Postprocessing.** Firstly, on each detected region is fitted an ellipse and the eccentricity factor is calculated. Region with eccentricity factor less than 1.1 are removed. Afterwards and in order to remove holes and artifacts we apply the same postprocessing used for SEM images, i.e., *removing holes and granularity* and *edge smoothing*.

### 3 Experiments and Discussion

In this section we discuss about different experiments using SEM and TEM images. The performance of the proposed algorithms is numerically evaluated by using real image databases. Based on these databases, which are manually segmented by an expert, we compute the overall accuracy measure in order to evaluate the efficiency of the proposal.

#### 3.1 Segmentation of SEM images.

For the experimental work we use 14 SEM images of size  $640 \times 430$  pixels. First row of Fig. 3 depicts examples of these images. Second row of Fig. 3 shows the results after applying the filter bank. Note that, the nanotube information have been significantly improved, even for the case with poor illumination, and the smooth illuminance variation in the background has also been removed.

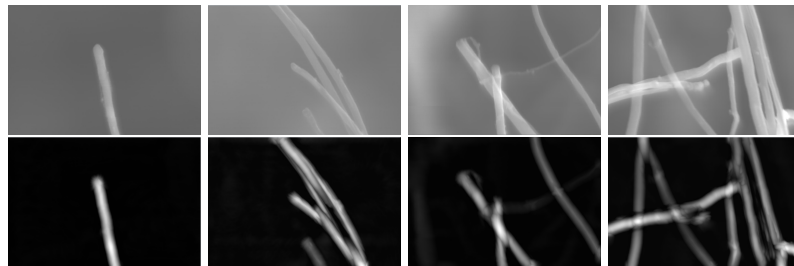


**Fig. 3.** Examples of SEM images. First row: (from left to right) real SEM images with different levels of complexity: easy, intermediate and difficult levels. Second row: corresponding preprocessed images after applying the Matched Filter Bank.

In order to train the multilayer neural network, we perform experiments with different feature vectors. First, we select patches that belong to nanotubes and non-nanotubes regions. In particular, the patches were taken from the image illustrated in the second row and third column in Fig. 3, see also Fig. 2. We carry out 5 experiments: one per each feature vector. The feature vectors are taken over pixels belonging to regions containing nanotubes and background. The explored features are: intensity levels of the image (Experiment I), vector composed by the local mean, variance and entropy (Experiment II), vector whose components include the intensity level and the local mean, variance and entropy (Experiment III), vector composed by the homogeneity, energy, contrast and correlation which are calculated from the co-occurrence matrix ( Experiment IV), vector whose components include the intensity level and the homogeneity, energy, contrast and correlation calculated from the co-occurrence matrix (Experiment V).

In order to assess the neural network we use the remaining 13 images. First row of Fig. 4 shows the result after applying the neural network with different

feature vectors. Second row of Fig. 4 shows the corresponding result after the postprocessing step. Observe the significant improvement of the postprocessing step for each executed experiment. The holes and discontinuities are removed and the body of nanotubes is recovered.

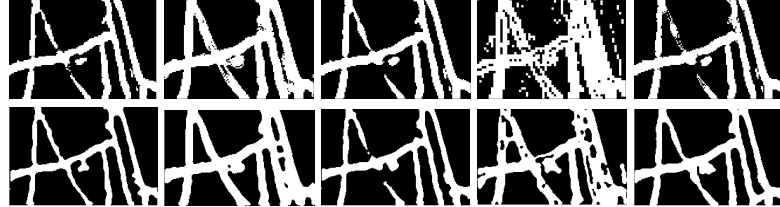


**Fig. 4.** Final result of the segmentation algorithm for SEM images. First row represents the outputs of the artificial neural network for the Experiments I, II, III, IV and V. Second row represents the results of the postprocessing step corresponding to the output of the artificial neural net (first row).

For numerically evaluating the performance of the proposed algorithm, see Section 2.2, we consider manually-segmented images by an expert. The third column of Table 3 shows a summary of the average of the overall accuracy computed over the 13 testing images. The evaluation considers the results of segmentation for the training and generalization phase after the postprocessing step. From the results in Table 3 we conclude that the neural network trained with the feature vector given by the intensity levels (Experiment I) leads to the best result.

**Table 3.** SEM images: Average of the Overall accuracy for the five executed experiments.

Experiment	Training (%)	Generalization (%)
<b>Experiment I</b>	<b>98.39</b>	<b>92.74</b>
Experiment II	95.58	89.92
Experiment III	97.15	92.42
Experiment IV	89.80	84.65
Experiment V	97.55	92.25

### 3.2 Segmentation of TEM images. Experiments

For the experimental work we use 41 TEM images, Fig. 5 shows examples of these images. All of them are manually segmented by an expert. As we can see, the images have different level of complexity: easy level when there is only one

nanotube; intermediate when there are two or more nanotubes; difficult level when there are overlaps between nanotubes, noise and the grid used is visible; very difficult level when they have the same problems as in images of difficult level and the nanotubes appear with interior holes. An example of the Preprocessing step is shown in Fig. 6.

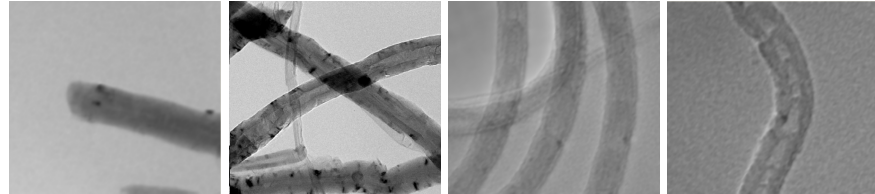


**Fig. 5.** Example of used TEM images. From left to right: images with easy, intermediate, difficult and very difficult levels

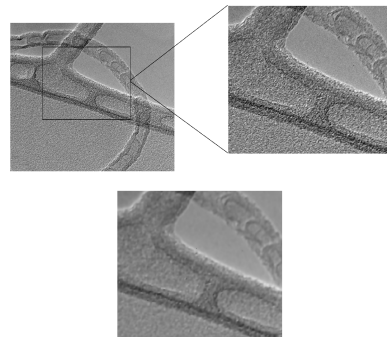


**Fig. 6.** Example of preprocessing step. The zoomed region contains the holes in the interior part of the nanotube and the background is very noisy (first row). The image is smoothed and the edges are preserved (second row).

Due to the complexity of the images, the neural network is applied per each image, i.e., the neural network is trained using pixels in the image with high confidence to belong to nanotube or background. Then the neural network is applied to pixels with low confidence to belong to the classes. For the previous reasons, the segmentation process for TEM images is more time consuming than for SEM images. In particular, the training process considers the 20 % of pixels falling in zones with high reliability (background and nanotube class according to expression (1)). In the generalization step the built networks classify pixels in uncertainty zones, see Eq. (1).

Similar to the experiments for SEM images, Subsection 3.1, we perform 5 experiments by using different feature vectors. Fig. 7 shows an example of the result for the segmentation process and postprocessing for each experiment. Note that, the postprocessing step allows us to eliminate small holes and to smooth edges. In order to assess the performance of the proposed algorithm, see Subsec-

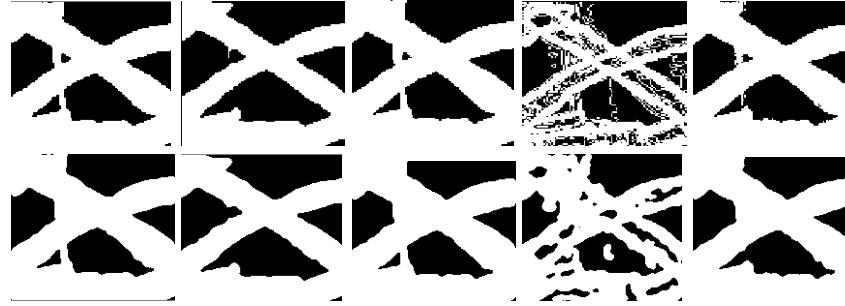


**Fig. 7.** Final result of the segmentation algorithm for TEM images. First row represents the outputs of the artificial neural network for the Experiments I, II, III, IV and V. Second row represents the results of the postprocessing step corresponding to the output of the artificial neural net (first row).

tion 2.3, we consider the 41 manually-segmented images by an expert. Table 4 gives a quantitative comparison of the average of the overall accuracy computed over these images. The evaluation includes the results of segmentation for the training and generalization phase and after the postprocessing step. According to the values in Table 4, we conclude that the feature vector of Experiment V, i.e., the feature vector that includes the intensity levels, the contrast, correlation, homogeneity and energy; yields the best results. Note that, the highest accuracy value is equal 73.99 %, which is less than the highest accuracy for SEM images (92.74%).

On the other hand, we note that the segmentation algorithm mainly misclassifies zones belonging to the background, which affects the overall accuracy. Some preliminary results show that if we increase the nanotube information in the learning process, the overall accuracy could also increase. For experiments in which the nanotechnologist indicates regions of interest, and then applies the whole algorithm, using the feature vector of Experiment V, one obtains an accuracy of 84.07%. This suggest that the algorithm can be used interactively, i.e., the expert selects a region of interest and then applies the segmentation algorithm. Fig. 8 illustrates an example of the previous experiment.

Finally, we note that most errors of this algorithm occur in images with poor illumination, with very granular texture, when the distribution of intensity levels of nanotube and background are very similar, or when the nanotube has interior holes. Fig. 9 depicts some examples of these images and the corresponding segmentation. According to the experimental work, we recommend a value of

**Table 4.** TEM images: Average of the Overall accuracy for the five executed experiments.

Experiment	Training (%)	Generalization (%)
Experiment I	85.74	70.32
Experiment II	85.43	60.65
Experiment III	<b>85.97</b>	69.38
Experiment IV	77.71	48.71
<b>Experiment V</b>	82.72	<b>73.99</b>

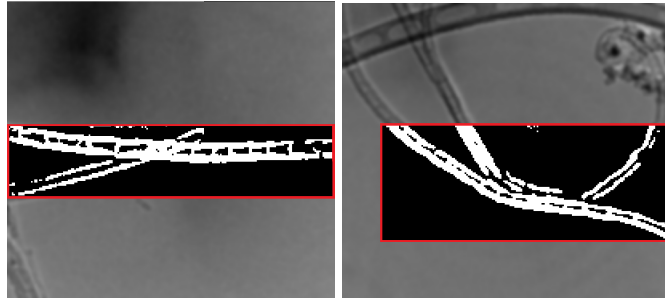


**Fig. 8.** Examples of segmented images using a region of interest given by an expert.

the relaxation parameter  $\theta$  in the interval [1, 2] for very noisy images, for less noisy images  $\theta$  can take values in the interval [3, 7]. When there are noticeable variations of intensity levels within classes,  $\theta$  can take values in the interval [15, 50].

#### 4 Conclusions

We proposed two algorithms for segmentation of carbon nanotube images: one for images obtained from Scanning Electron Microscopy and the other for segmenting images from Transmission Electron Microscopy. Both algorithms consider three steps: preprocessing, segmentation and postprocessing. The preprocessing step allowed to increase the contrast between nanotube and background using appropriate filters. The segmentation stage is based on a neural network approach. For TEM images a threshold technique is included with the goal of detecting regions of high confidence to belong to nanotube or background classes, which are considered as training data for the neural network. Due to the complexity of carbon nanotube images a postprocessing step was required with the aim of removing artifacts, such that holes inside nanotubes and granularities. The performance of both algorithms was evaluated using real image databases, which were manually segmented by an expert. According to the experimental work the segmentation of SEM images obtained an excellent accuracy. On the other hand, the accuracy of the algorithm for TEM images was good, although, it can be improved if an expert selects regions of interest in the image. The performance

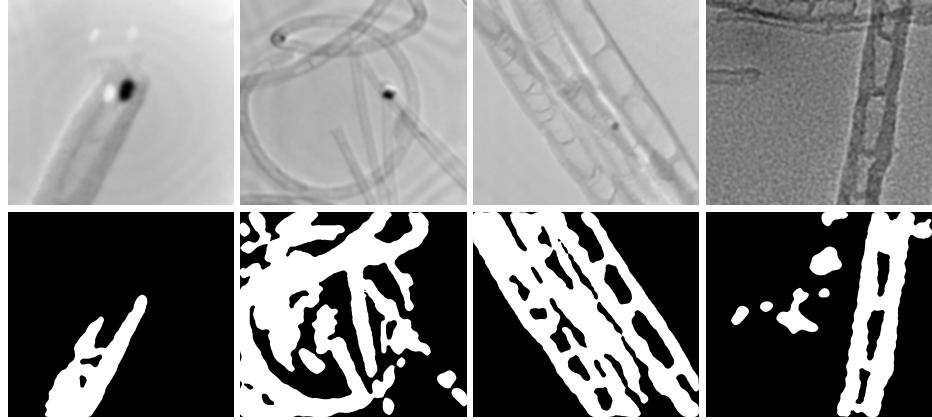


**Fig. 9.** Examples of segmentation results with errors due to the complexity of the image.

of the method was sensitive to the holes inside nanotubes and artifacts like the grid used in the synthesis for TEM images.

## Acknowledgments

This research was partially supported by the Project PROMEP/103.5/11/6834.

## References

1. Aguilar, O., Alarcón, T., Dalmau, O., Zamudio, A.: Characterization of nanotube structures using digital-segmented images. In: Thirteenth Mexican International Conference on Intelligence Special Session, Revised Papers. pp. 53–61. IEEE Computer Society (2014)
2. Batenburg, K.J., Sijbers, J.: Adaptive thresholding of tomograms by projection distance minimization. *Pattern Recognition* 42(10), 2297?2305 (2009)
3. Bates, D.M., Watts, D.G.: Nonlinear regression: iterative estimation and linear approximations. Wiley Online Library (1988)
4. Chaku, P., Shah, P., Bakshi, S.: A digital image processing algorithm for automation of human karyotyping. *International Journal of Computer Science and Communication (IJCSC)* 5(1), 54–56 (March-Sep 2014)
5. Chaudhuri, S., Chatterjee, S., Katz, N., Nelson, M., Goldbaum, M.: Detection of blood vessels in retinal images using two-dimensional matched filters. *EEE Transactions on Medical Imaging* 8(3), 263–269 (1989)
6. Chuang, K.S., Tzeng, H.L., Chen, S., Wu, J., Chen, T.J.: Fuzzy c-means clustering with spatial information for image segmentation. *Computerized Medical Imaging and Graphics* 30, 9?15 (2006)
7. Dalmau, O., Alarcon, T.: MFCA: Matched filters with cellular automata for retinal vessel detection. In: MICAI 2011, Part I, LNAI 7094. pp. 504–514. Springer-Verlag Berlin Heidelberg (2011)

8. Gao, Y., Li, Z., Lin, Z., Zhu, L., Tannenbaum, A., Bouix, S., Wong, C.: Automated dispersion and orientation analysis for carbon nanotube reinforced polymer composites. *Nanotechnology* 23(43) (2012)
9. Geman, S., Geman, D.: Stochastic relaxation, gibbs distributions and bayesian restoration of images. *IEEE Transactions on Pattern Analysis and Machine Intelligence* 6(6), 721–741 (2004)
10. Gill, P.R., Murray, W., Wright, M.H.: *The Levenberg-Marquardt Method. Practical Optimization*, London: Academic Press (1981)
11. Gonzalez, R., Woods, R.: *Digital image processing*. Pearson/Prentice Hall (2008), <http://books.google.com.mx/books?id=8uG0njRGEzoC>
12. Haralick, R.M., Shanmugam, K., Dinstein, I.: Textural features for image classification. *EEE Transactions on Systems, Man, and Cybernetics* 3(6), 610?621 (1973)
13. de Jes  es Guerrero Casas, J., Dalmau, O., Alarc  n, T.E., Zamudio, A.: Frequency filter bank for enhancing carbon nanotube images. In: *MICAI 2014, Part I, LNAI 8856*. pp. 316–326. Springer International Publishing Switzerland (2014)
14. Levenberg, K.: A Method for the Solution of Certain Problems in Least Squares. *Quart. Appl. Math* (1944)
15. Lindeberg, T., Li, M.X.: Segmentation and classification of edges using minimum description length approximation and complementary junction cues. *Computer Vision and Image Understanding* 67, 88–98 (1997)
16. Nock, R., Nielsen, F.: Statistical region merging. *IEEE Transactions on Pattern Analysis and Machine Intelligence* 26, 1452–1458 (2004)
17. Otsu, N.: A threshold selection method from gray-level histogram. *IEEE Transactions on System Man Cybernetics vol. SMC-9(1)* (1979)
18. Perona, P., Malik, J.: Scale-space and edge detection using anisotropic diffusion. *Pattern Analysis and Machine Intelligence, IEEE Transactions on* 12(7), 629–639 (1990)
19. Rajaraman, S., Vaidyanathan, G., Chokkalingam, A.: Segmentation and removal of interphase cells from chromosome images using multidirectional block ranking. *International Journal of Bio-Science and Bio-Technology* 5(3), 79–91 (June 2013)
20. Shapiro, L.G., Stockman, G.C.: *Computer Vision*. Prentice-Hall (2001)
21. Torres, A.D.: *Procesamiento digital de im  genes*. Perfiles Educativos pp. 1–15 (abril-junio 1996)